Analyst

RSC Publishing

PAPER

View Article Online
View Journal | View Issue

Cite this: *Analyst*, 2013, **138**, 6463

Human cytochrome P450 3A4 and a carbon nanofiber modified film electrode as a platform for the simple evaluation of drug metabolism and inhibition reactions†

Qiang Xue,[a] Dai Kato,[a] Tomoyuki Kamata,[a] Qiaohui Guo,[b] Tianyan You[b] and Osamu Niwa*[a]

Received 9th July 2013
Accepted 13th August 2013

DOI: 10.1039/c3an01313h

www.rsc.org/analyst

Electrochemical biosensors consisting of cytochrome P450 enzyme modified electrodes have been developed to provide a simple method for screening the metabolism of a drug and its inhibitor. Here, we report a very simple electrochemically driven biosensor for detecting drug metabolism and its inhibition based on cytochrome P450 3A4 (CYP3A4) and a carbon nanofiber (CNF) modified film electrode without any other modified layers such as mediator films. Direct electron transfer (DET) between CYP3A4 and CNFs was observed at a formal potential of −0.302 V. The electrocatalytic reduction current increased with the addition of drugs including testosterone and quinidine. In contrast, the reduction current was greatly suppressed in the presence of ketoconazole, which is a CYP3A4 inhibitor. CNFs with high conductivity, a large surface area and sufficient edge planes provide a suitable microenvironment for achieving excellent DET and biocatalysis properties, which could not be observed when we used other carbon materials such as carbon nanotube (CNT) and carbon black (CB) modified electrodes, indicating that our system is promising as a new bioelectronic platform for electrochemical biosensing.

Introduction

Human cytochrome P450 3A4 (CYP3A4) is deemed to be the most significant enzyme in the P450 family for drug metabolism.[1] CYP3A4 metabolizes more drug molecules than all other isoforms combined[2] and it plays a crucial role in the metabolism of 50% of clinical drugs. Therefore, the development of a simple and rapid method for screening drug candidates by detecting changes in CYP3A4 activity is significant as regards metabolism and inhibition. Traditionally, the activity of CYP3A4 is determined from the rate at which metabolites are formed by the donation of electrons from NADPH to CYP3A4.[3] Since the commonly used HPLC and photometric analysis methods are expensive and time-consuming, much simpler and less expensive methods have been developed. Previous reports indicated that the electrode could be employed as an alternative source of electrons, instead of NADPH, for electrochemically driven catalysis of P450 enzymes.[4–6] In recent years, electrochemical enzyme sensors based on the direct electron transfer (DET) between CYP3A4 and an electrode have been studied to realize the simple detection of drug metabolites, because they do not require expensive NADPH and its regenerating enzymes. Joseph *et al.* reported the direct electrochemistry of CYP3A4 and its biocatalysis of four substrates (verapamil, midazolam, quinidine, and progesterone) at a poly(dimethyldiallylammonium chloride) (PDDA) and 3-mercapto-1-propenesulfonic acid (MPS) modified gold electrode.[7] Gilardi and co-workers have found that DET was obtained at thiol reactive cystamine–maleimide modified gold and polyion modified glassy carbon (GC) electrodes, and artificial redox chains were employed to enhance the coupling efficiency and catalytic activity of CYP3A4.[8]

More recently, Mie *et al.* obtained DET at a gold electrode modified with hydrophobic layers of aromatic compounds. They indicated that the electrochemically driven metabolism of testosterone was detected at the CYP3A4 microsome modified electrode.[9] Liu's group also achieved DET at a Au electrode modified with CYP3A4/CPR microsomes using modified hybrid layers (nanocomposites consist of PDDA functionalized graphene sheets and gold nanoparticles).[10] All of the above studies have used modified layers including polyelectrolyte or naphthalenethiolate to provide a suitable biomembrane-like microenvironment for immobilizing proteins and accelerating electron transfer. It has been reported that the direct electrochemistry of CYPs at an electrode without modified layers is very difficult.[11] Therefore, the efficient DET of CYP3A4 without a modified layer is still a challenging target if we are to realize

[a]*National Institute of Advanced Industrial Science and Technology (AIST), Higashi, Tsukuba, Ibaraki 305-8566, Japan. E-mail: niwa.o@aist.go.jp*

[b]*The State Key Laboratory of Electroanalytical Chemistry, Changchun Institute of Applied Chemistry, Chinese Academy of Sciences, Changchun 130022, PR China*

† Electronic supplementary information (ESI) available. See DOI: 10.1039/c3an01313h

simpler drug metabolism sensors. Electrode materials play a significant role in achieving efficient DET of enzymes.[5,12,13] Carbon nanomaterials are promising as candidate electrode materials for the direct electrochemistry of enzymes because of their wide variety of chemical structures and morphology, which is beneficial in terms of reducing the distance between the enzyme redox center and the electrode surface.

Previous reports have shown that carbon nanotubes (CNTs) and carbon nanofibers (CNFs) can provide a suitable microenvironment for obtaining the DET of redox proteins such as glucose oxidase, laccase, bilirubin oxidase and cytochrome c,[14–18] because they have large surface areas that can provide a suitable nanospace so that the redox center of the enzymes is close to the electrode surface. Although both CNTs and CNFs have great mechanical strength, excellent electrical conductivity, and biocompatibility, CNFs are less ordered materials and have more edge planes on their sidewalls than CNTs,[19,20] which may facilitate electron transfer. This also suggests that the CNF sidewalls would be more suitable for biomolecule (such as enzyme) adsorption. In addition, CNFs can be synthesized without any catalyst involved in the carbonization process. These unique characteristics are beneficial for designing an electrochemical enzyme biosensor based on DET.

In this study, we investigated an electrochemically driven CYP3A4 biosensor based on DET by employing a CNF modified film electrode without using an organic (or polymeric) modified layer. We also compared the electrocatalytic activities of CYP3A4 when co-immobilized with different carbon nanomaterials such as CNTs and carbon black (CB). A CYP3A4 and CNF (CYP3A4/CNF) modified film electrode exhibited a more effective dioxygen reduction current than CNT and CB modified film electrodes. The metabolism of testosterone and quinidine and its inhibition with ketoconazole were detected using a CYP3A4/CNF modified film electrode with the same quality of electrode response as that of previously reported CYP3A4 modified electrodes using organic (or polymeric) modified layers.

Experimental

Materials and apparatus

All of the chemicals employed in this study were of analytical grade and used as received without further purification. Purified human CYP3A4 was purchased from Cypex Ltd. (UK). Ketoconazole, testosterone and quinidine were purchased from Wako Pure Chemical Industries Ltd. (Japan). Phosphate buffer solution (PB, 0.1 M, pH 7.0) was prepared by mixing stock solutions of Na_2HPO_4 and NaH_2PO_4. The CNFs were fabricated using a previously reported electrospinning method.[21] Multiwall carbon nanotubes (MWCNTs, diameter 110–170 nm, fabricated with the chemical vapor deposition (CVD) method) were purchased from Sigma-Aldrich Co. Carbon black (CB, mean size 110 nm) was purchased from Tokai Carbon Co., Ltd. (Aqua-Black, Japan). Highly oriented pyrolytic graphite (HOPG) electrodes (edge plane and basal plane) were purchased from BAS Co. (Tokyo, Japan). The morphologies of the electrode surfaces were evaluated with a field-emission scanning electron microscope (FE-SEM, S4800, Hitachi, Japan) and an atomic force microscope (AFM, SPM-9600, Japan). Raman spectra were acquired using a Raman microspectrometer (DXR Raman Microscope, Japan) equipped with an optical microscope under ambient conditions and using a 780 nm laser.

Preparation of a CNF modified film electrode

Nanocarbon films deposited by the unbalanced magnetron sputtering (UBMS) method were used as base film electrodes because a UBMS nanocarbon film has a wide potential window in the cathodic region that is suitable for measuring the oxygen reduction current based on DET with a high *S*/*N* ratio. The film also provides relatively good electrochemical properties similar to those of our previously reported nanocarbon film formed by electron cyclotron resonance (ECR) sputtering.[22] After depositing the nanocarbon film on the Si wafer, we cut the carbon material into rectangles, and then fixed a plastic tape with a 2 mm diameter hole in it onto these nanocarbon films to form disk electrodes. The fabrication process of the CNF modified film electrode was based on our previous report.[23] Briefly, CNFs were crushed into powder and dispersed in water *via* energetic mixing and then sonicated for 60 min to form a CNF solution (1 mg mL^{-1}). The CNF modified film electrodes were prepared by casting 6 μL of CNF solution onto the surface of the UBMS nanocarbon film and then drying it at room temperature. Other electrodes modified with carbon materials were prepared in the same way except for the process described below that was used for CNT purification. Before casting the CNT solution onto the electrode surface, the solution was centrifuged at 12 000 rpm to remove impurities (including the catalyst). This operation was repeated three times.

Electrochemical measurements for CYP3A4

Purified CYP3A4 was dissolved in a PB solution. To achieve physical adsorption of CYP3A4 onto the CNF modified film electrode surface, we cast 5 μL of CYP3A4 solution (20 μM) onto the electrode surface. After incubation for 30 min at 25 °C, the prepared enzyme electrode was rinsed with PB solution. The enzyme modified electrode was then transferred to a PB solution to evaluate the DET and the electrocatalytic and inhibition properties.

All electrochemical measurements were performed with an ALS/CHI 730C electrochemical analyzer (CH Instruments, Inc., USA). A conventional three-electrode configuration was used. The prepared electrode was used as the working electrode. An Ag/AgCl (3 M NaCl) electrode and a Pt wire served as reference and auxiliary electrodes, respectively.

Results and discussion

Characterization of CNFs

We characterized the surface properties of the CNF by SEM, AFM and Raman spectrometry. Fig. 1a shows an image of the pristine CNF, which is black and cotton-like in appearance. The CNFs are regular and fibrous with a network-like morphology (Fig. 1b and c). The diameter is 200–400 nm and the length after crushing is several micrometers. The

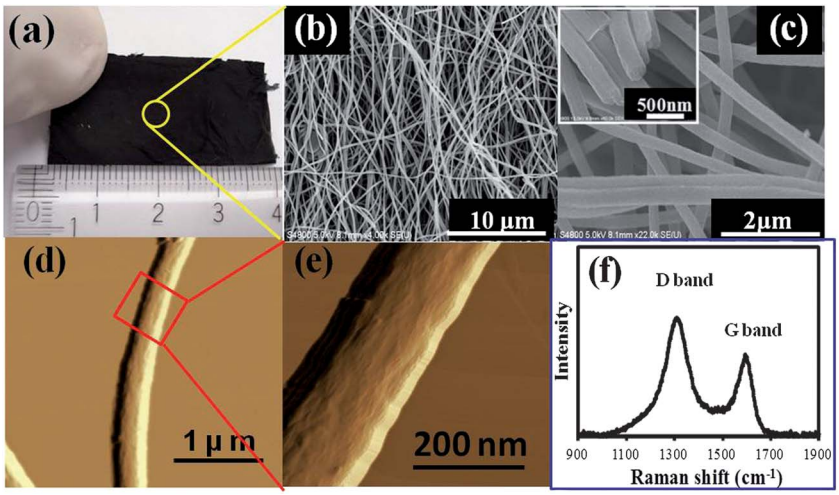

Fig. 1 Characterization of the CNF. (a) Image of the as-grown CNF, (b and c) SEM images of a CNF at low and high magnifications, (d and e) AFM images of a CNF at different resolutions, and (f) Raman spectrum of a CNF.

morphology of a single CNF as revealed by the AFM images indicated that it was rod shaped with a rough surface (the average roughness is 4 nm), as shown in Fig. 1d and e. The microstructure of the CNF was characterized by Raman spectroscopy. Fig. 1f shows two distinct peaks at 1302 and 1592 cm^{-1}, which are defined as the D (disordered turbostratic carbon structure) and G bands (ordered graphitic structure), respectively.[24,25] The relative intensity ratio of the D band to the G band ($R = I_D/I_G$) reflects the number of defect sites present in the carbon materials.[21] The R value of CNFs is 1.47 which is larger than that of other nanocarbon materials such as MWCNTs (0.999) and graphene sheets (1.02).[21,26] It has been reported that an R value greater than 1.0 indicates a highly disordered structure with the presence of many defects in the graphitic structure,[27] which suggests that there are a large number of edge-plane defect sites in the CNFs. Since it has been reported that the edge-plane defects displayed high electrocatalytic activity in relation to certain biomolecules,[21] a large number of edge-plane defect sites are beneficial as regards electrochemical activity.

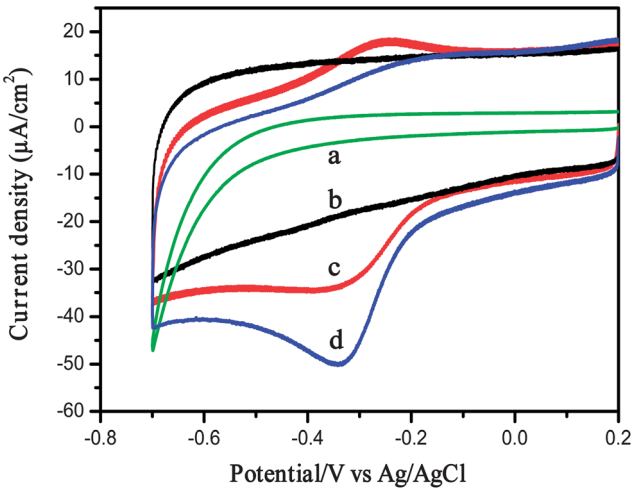

Fig. 2 Cyclic voltammograms showing the direct electrochemistry of CYP3A4 at various CNF modified electrodes: (a) CYP3A4 modified film electrode; (b) CNF modified film electrode; (c) CYP3A4/CNF modified film electrode (a–c: anaerobic condition, argon purge for at least 30 min and maintained in an argon atmosphere); (d) CYP3A4/CNF modified film electrode (aerobic condition, argon purge for 10 min). Scan rate: 150 mV s^{-1}; PB solution (0.1 M, pH 7.0).

Direct electrochemistry of CYP3A4

Although it is very difficult to achieve the DET of CYP at an electrode without any modification layers, one of the most promising technologies for its successful realization involves the use of an electrode material with a suitable nanostructured surface. Here, we examined the DET properties of a CYP3A4/CNF modified film electrode without any modification layer. No redox peaks were observed at the CYP3A4 modified film electrode (Fig. 2, curve a) or the CNF modified film electrode (Fig. 2, curve b). In contrast, the CYP3A4/CNF modified film electrode clearly exhibited redox waves at −0.260 and −0.344 V *vs.* Ag/AgCl in an anaerobic solution (Fig. 2, curve c). Moreover, the reduction peak was increased 1.5 times under aerobic conditions, and the oxidation peak disappeared completely as shown in Fig. 2 (curve d), suggesting a typical electrocatalytic oxygen reduction process based on the fast binding of oxygen to the reduced ferrous cytochrome P450,[7,10,28] and then rapid electron transfer between the enzyme and electrode. Therefore, the response current was obviously due to the DET-type electrocatalytic reaction between an enzyme active center and the electrode surface. It is noteworthy that DET from a CYP protein was achieved at the CYP3A4/CNF modified film electrode without any other modified layers, thus confirming that the CNF is a very significant electrode material for the DET of CYP3A4. This excellent DET characteristic could be due to the favorable microenvironment for CYP3A4 immobilization created by CNFs with high conductivity, a large surface area and abundant edge-plane defect sites.

The formal potential (mid-point potential) at the CYP3A4 modified electrode was −0.302 V, which was almost the same as

a previously reported value for purified CYP3A4 (−0.319 V *vs.* Ag/AgCl).[29] This formal potential was positively shifted compared with the reported value (−0.40 V *vs.* Ag/AgCl) for CYP3A4/CPR-microsomes on a naphthalenethiolate modified gold electrode,[9] and the value (−0.482 V *vs.* SCE) for CYP3A4/CPR-microsomes on a gold–graphene nanocomposite modified gold electrode.[10] The difference could be attributed to the distinct microenvironment induced by the CYP3A4/CNF modified film electrode without any modified layer, since it is known that an electrode surface material and modification can alter the microenvironment for cyt P450s and affect the reduction potentials of P450s.[8,30]

Comparison of the electrocatalytic performance of CYP3A4 at various electrodes

Other carbon nanomaterials including CB and CNT modified film electrodes were also studied to compare the catalytic currents of CYP3A4. In Fig. 3a, a clear response current was obtained at the CYP3A4/CNF modified film electrode as described above (red line). In contrast, we observed only a slight response current at the CYP3A4/CNT modified film electrode as shown in Fig. 3b (pink line). This was because the CNT sidewall was less electroactive than that of CNFs, although they both have excellent electronic properties and large surface areas. It has been reported that CNFs are less ordered materials and have more edge planes on their sidewalls than CNTs.[19,20] Tominaga *et al.* indicated that the electrochemical properties of the MWCNT sidewalls could be similar to those of the basal plane of HOPG and are essentially inert. His group also reported that edge-plane-like defects, including the open ends in MWCNTs or the step edge, dominate the electrochemical properties.[31] We also measured the electrocatalytic performance of CYP3A4 modified HOPG (basal and edge plane) electrodes, and the results showed that a higher response current was achieved at the edge plane HOPG electrode (Fig. S1†). This result also supported the idea that an electrode based on CNFs, which has sufficient edge planes on its sidewalls, exhibits better DET than a CNT based electrode.

In Fig. 3c, no catalytic current peak can be seen at the CYP3A4 and CB (CYP3A4/CB) modified film electrode despite the fact that it exhibited the largest capacitance (black line). Since the edge plane of carbon has a high electrochemical activity for biomolecules,[22] and CB is a form of amorphous carbon,[32] the absence of the response current at the CYP3A4/CB modified electrode could be due to the lower edge plane content as a result of their amorphous structure. Therefore, the CYP3A4/CNF modified film electrode can provide better conditions for achieving efficient direct electrocatalytic current than those at other film electrodes modified with carbon materials when we do not use modified layers such as mediators.

Drug metabolism and its inhibition at the CYP3A4/CNF modified film electrode

We confirmed efficient DET at the CYP3A4/CNF modified film electrode as described above, and so we anticipate that electrochemically driven drug metabolism and inhibition reactions can be achieved by using the CYP3A4/CNF modified film electrode. A model of the drug metabolism and its related inhibition process is shown schematically in Fig. 4. Fig. 5 shows the effect of typical substrates (drugs: testosterone and quinidine) and inhibitor (ketoconazole) on the electrocatalytic current of CYP3A4. In Fig. 5a and b, catalytic currents were clearly observed in the absence of substrates (blue lines). When 200 μM of testosterone or quinidine was added to the system, an increased reduction current was observed (red lines), which indicated that the drug metabolism reaction occurred effectively. The difference between the peak potential shifts for the metabolism of the two substrates might result from different binding sites with the enzyme and the related distinct drug metabolism mechanism, since the presence of multiple binding sites within the CYP3A4 active site has been indicated by several studies.[33,34] The reduction peak negatively shifted only after the addition of quinidine. This could be an implication of the lower electron transfer for the quinidine metabolism than that for the testosterone metabolism, since we obtained smaller apparent Michaelis–Menten constant (K_m^{app}) for the testosterone metabolism than that for the quinidine metabolism, as shown in the later section. In addition, it has been reported that quinidine is

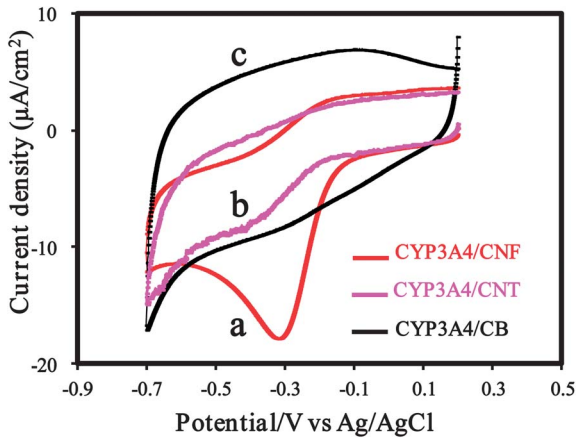

Fig. 3 Comparison of the electrocatalytic performance of CYP3A4 at various carbon material modified film electrodes. (a) CYP3A4/CNF modified film electrode, (b) CYP3A4/CNT modified film electrode, and (c) CYP3A4/CB modified film electrode. Scan rate: 20 mV s^{-1}; PB solution (0.1 M, pH 7.0).

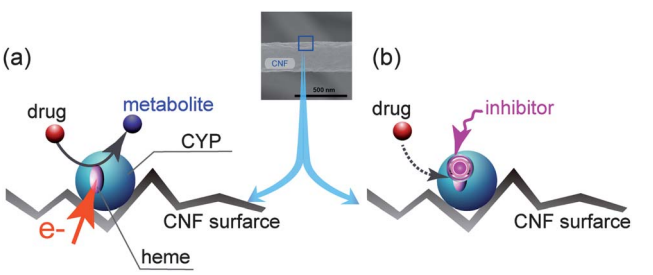

Fig. 4 Schematic illustration of drug metabolism and the related inhibition process at the CYP3A4/CNF modified film electrode. (a) Drug metabolism and (b) enzyme inhibition.

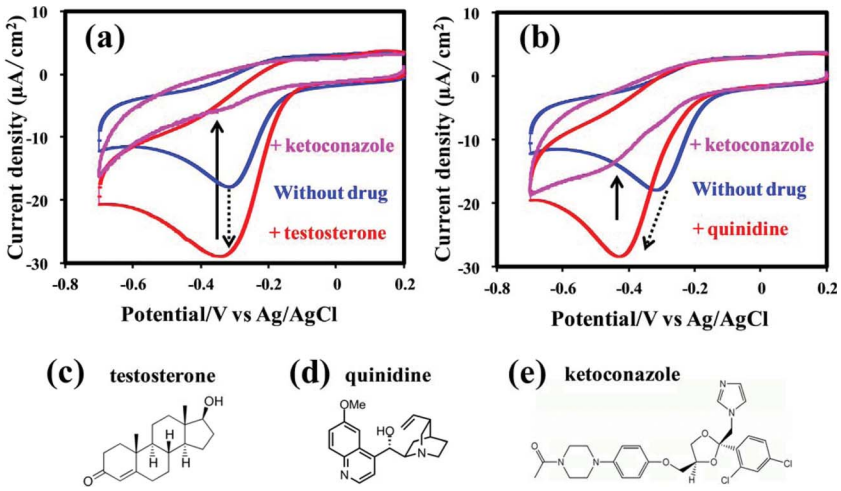

Fig. 5 Electrocatalysis behavior (effect of substrate and inhibitor) at the CYP3A4/CNF modified film electrode. Scan rate: 20 mV s^{-1}; PB solution (0.1 M, pH 7.0). Substrates (testosterone and quinidine): 200 μM and inhibitor (ketoconazole): 200 μM. (a) Testosterone metabolism and its inhibition, (b) quinidine metabolism and its inhibition, and (c–e) substrates and inhibitor used in this study.

not only a substrate but also an inhibitor for CYP3A4.[35] The efficiency of this CNF-based biosensor was evaluated in terms of the ratio of the catalyzed current of the substrate (drug) (I_{cat}(substrate)) to the oxygen reduction current ($I_{cat}(O_2)$). The I_{cat}(substrate)/$I_{cat}(O_2)$ values for testosterone and quinidine are 1.63 and 1.59, respectively, which are larger than those of a previous reported CYP3A4 biosensor containing a PDDA layer (1.38).[7] This result indicated that our CYP3A4/CNF modified film electrode provided a suitable environment for a high catalytic ability even without a modified layer. Based on the Michaelis–Menten equation, the apparent K_m^{app} values, calculated from the relationship between catalytic currents and concentrations of drugs (testosterone and quinidine), were 8.9 and 14.1 μM for testosterone and quinidine, respectively. These values are lower than the values described in other reports,[9,36] which infer that a good affinity of CYP3A4-substrate activity was obtained in our system (Fig. S2†). This is highly advantageous for constructing these kinds of biosensors with a simple configuration. Ketoconazole was used to evaluate the inhibition effect on the metabolic activity of CYP3A4. When 200 μM ketoconazole was introduced into the system, the reduction currents were significantly decreased (pink lines). The inhibition efficiencies for testosterone and quinidine metabolism were 81.3% and 52.8%, respectively. This result clearly showed that the inhibition of enzyme activity by ketoconazole could be efficiently detected. The IC_{50} value was used to describe the more detailed enzyme inhibition effect in the presence of testosterone (Fig. S3†). The inhibition data followed a binomial model ($Y = 2 \times 10^{-05}X^2 - 0.0072X + 0.8573$), and the IC_{50} value was calculated to be 58.5 μM. The inhibition effect on testosterone metabolism was similar to that of a previous report.[9] These results are essential in terms of obtaining a further understanding of the drug metabolism mechanism and the related inhibition reaction at the CNF based electrode. We are now exploring ways of using our CNF based electrode in relation to the metabolism of other drugs and the related inhibition reaction or the properties of other CYPs.

Conclusion

We successfully achieved efficient DET at a CYP3A4/CNF modified film electrode without any modification layers such as mediators. Compared with other carbon nanomaterials such as CNTs and CB, the CYP3A4/CNF modified film electrode exhibits a much larger and sharper electrocatalytic current for oxygen reduction. The CYP3A4/CNF modified film electrode also allowed us to evaluate electrochemically driven drug metabolism and its inhibition by simply measuring the magnitude of reduction currents. In fact, the reduction currents increased 1.63 and 1.59 times when we added testosterone and quinidine, respectively and also decreased 81.3% and 52.8% when we added a ketoconazole inhibitor. The apparent K_m^{app} values were 8.9 and 14.1 μM for testosterone and quinidine, respectively. These results show the potential for developing a much simpler and more sophisticated drug screening biosensor platform based on CNFs. We will now focus on extending this system to the metabolism of a wide variety of drugs and for screening its inhibitors.

Acknowledgements

This work was supported in part by a Grant-in-Aid for Scientific Research (O.N. no. 23350038) from MEXT, Japan. This work was carried out in part at the Nano-Processing Facility, supported by AIST, Japan.

References

1 G. Luo, M. Cunningham, S. Kim, T. Burn, J. Lin, M. Sinz, G. Hamilton, C. Rizzo, S. Jolley and D. Gilbert, *Drug Metab. Dispos.*, 2002, **30**, 795–804.
2 P. A. Williams, J. Cosme, D. M. Vinković, A. Ward, H. C. Angove, P. J. Day, C. Vonrhein, I. J. Tickle and H. Jhoti, *Science*, 2004, **305**, 683–686.
3 J. E. McGraw Sr and D. P. Waller, *Biochem. Biophys. Res. Commun.*, 2006, **344**, 129–133.

4 S. Liu, L. Peng, X. Yang, Y. Wu and L. He, *Anal. Biochem.*, 2008, **375**, 209–216.
5 X. Xu, W. Wei, M. Huang, L. Yao and S. Liu, *Chem. Commun.*, 2012, **48**, 7802–7804.
6 L. Peng, X. Yang, Q. Zhang and S. Liu, *Electroanalysis*, 2008, **20**, 803–807.
7 S. Joseph, J. F. Rusling, Y. M. Lvov, T. Friedberg and U. Fuhr, *Biochem. Pharmacol.*, 2003, **65**, 1817–1826.
8 V. R. Dodhia, C. Sassone, A. Fantuzzi, G. D. Nardo, S. J. Sadeghi and G. Gilardi, *Electrochem. Commun.*, 2008, **10**, 1744–1747.
9 Y. Mie, M. Suzuki and Y. Komatsu, *J. Am. Chem. Soc.*, 2009, **131**, 6646–6647.
10 M. Huang, X. Xu, H. Yang and S. Liu, *RSC Adv.*, 2012, **2**, 12844–12850.
11 S. J. Sadeghi, A. Fantuzzi and G. Gilardi, *Biochim. Biophys. Acta*, 2011, **1814**, 237–248.
12 H. Liu, Y. Tian and P. Xia, *Langmuir*, 2008, **24**, 6359–6366.
13 D. Cao, P. He and N. Hu, *Analyst*, 2003, **128**, 1268–1274.
14 A. Guiseppi-Elie, C. H. Lei and R. H. Baughman, *Nanotechnology*, 2002, **13**, 559–564.
15 Y. Liu, M. Wang, F. Zhao, Z. Xu and S. Dong, *Biosens. Bioelectron.*, 2005, **21**, 984–988.
16 Q. L. Sheng, J. B. Zheng, X. D. Shang-Guan, W. H. Lin, Y. Y. Li and R. X. Liu, *Electrochim. Acta*, 2010, **55**, 3185–3191.
17 Y. Yan, W. Zheng, L. Su and L. Mao, *Adv. Mater.*, 2006, **18**, 2639–2643.
18 F. Gao, Y. Yan, L. Su, L. Wang and L. Mao, *Electrochem. Commun.*, 2007, **9**, 989–996.
19 X. Lu, J. Zhou, W. Lu, Q. Liu and J. Li, *Biosens. Bioelectron.*, 2008, **23**, 1236–1243.
20 V. Vamvakaki, K. Tsagaraki and N. Chaniotakis, *Anal. Chem.*, 2006, **78**, 5538–5542.
21 Y. Liu, J. Huang, H. Hou and T. You, *Electrochem. Commun.*, 2008, **10**, 1431–1434.
22 A. Ueda, D. Kato, R. Kurita, T. Kamata, H. Inokuchi, S. Umemura, S. Hirono and O. Niwa, *J. Am. Chem. Soc.*, 2011, **133**, 4840–4846.
23 Q. Xue, D. Kato, T. Kamata, Q. Guo, T. You and O. Niwa, *Anal. Sci.*, 2013, **29**, 611–618.
24 Y. Lin, K. A. Watson, M. J. Fallbach, S. Ghose, J. G. Smith Jr, D. M. Delozier, W. Cao, R. E. Crooks and J. W. Connell, *ACS Nano*, 2009, **3**, 871–884.
25 R. L. McCreery, *Chem. Rev.*, 2008, **108**, 2646–2687.
26 Z.-J. Fan, J. Yan, T. Wei, G.-Q. Ning, L.-J. Zhi, J.-C. Liu, D.-X. Cao, G.-L. Wang and F. Wei, *ACS Nano*, 2011, **5**, 2787–2794.
27 S. Maldonado and K. J. Stevenson, *J. Phys. Chem. B*, 2004, **108**, 11375–11383.
28 V. V. Shumyantseva, Y. D. Ivanov, N. Bistolas, F. W. Scheller, A. I. Archakov and U. Wollenberger, *Anal. Chem.*, 2004, **76**, 6046–6052.
29 S. J. Sadeghi, S. Ferrero, G. Di Nardo and G. Gilardi, *Bioelectrochemistry*, 2012, **86**, 87–91.
30 A. K. Udit, N. Hindoyan, M. G. Hill, F. H. Arnold and H. B. Gray, *Inorg. Chem.*, 2005, **44**, 4109–4111.
31 M. Tominaga, S. Sakamoto and H. Yamaguchi, *J. Phys. Chem. C*, 2012, **116**, 9498–9506.
32 C. H. An Wong, A. Ambrosi and M. Pumera, *Nanoscale*, 2012, **4**, 4972–4977.
33 K. Korzekwa, N. Krishnamachary, M. Shou, A. Ogai, R. Parise, A. Rettie, F. Gonzalez and T. Tracy, *Biochemistry*, 1998, **37**, 4137–4147.
34 M. Shou, R. Dai, D. Cui, K. R. Korzekwa, T. A. Baillie and T. H. Rushmore, *J. Biol. Chem.*, 2001, **276**, 2256–2262.
35 C. C. Ogu and J. L. Maxa, *Proc. (Bayl. Univ. Med. Cent.)*, 2000, **13**, 421–423.
36 V. Agrawal, J. H. Choi, K. M. Giacomini and W. L. Miller, *Pharmacogenet. Genomics*, 2010, **20**, 611–618.